25th Australasian Conference on Mechanics of Structures and Materials (ACMSM25)
Edited by C.M. Wang, J.C.M. Ho and S. Kitipornchai
Brisbane, Australia, December 4 – 7, 2018

FLEXURAL BEHAVIOUR OF FUNCTIONALLY GRADED-GRAPHENE REINFORCED COMPOSITE PLATES

M.R.R. RASAPPAGARI[1, 3], W. KARUNASENA[1, 2,*] and W. LOKUGE[1, 2]

[1]School of Civil Engineering and Surveying, University of Southern Queensland, QLD 4350, Australia

[2]Centre for Future Materials, University of Southern Queensland, Toowoomba, QLD 4350, Australia

[3]School of Natural and Built Environments, University of South Australia, Adelaide, SA 5095, Australia

Emails: muniramireddyrasappagari@gmail.com, karu.karunasena@usq.edu.au, weena.lokuge@usq.edu.au
*Corresponding author

Abstract. *A first order shear deformation theory based finite element numerical investigation on flexure behaviour of functionally graded thin, moderately thick and thick composite plates reinforced with graphene platelets (GPLs) is presented in this paper. The maximum deflection plays a major role in the design of composite structures. Therefore, maximum deflection and percentage maximum deflection ratio of reinforced to unreinforced composite plate are investigated for a range of GPL distribution patterns along plan and thickness directions of the composite plate. Modified Halpin-Tsai equation is used to determine the effective Young's modulus for each layer in thickness direction for different distribution patterns. The rule of mixture is used to calculate effective mass density and Poisson's ratio for each layer. Initially, the results from this study are verified by comparing with the reported results from the literature. Thereafter, validated methodology is used to conduct case study for a simply supported plate, focusing on the effect of thickness, GPL distribution patterns along plan and thickness directions, percentage weight fraction of GPL on the maximum deflection and percentage maximum deflection ratio of reinforced to unreinforced composite plate. It is found that by adding just 1% weight fraction of GPL, the maximum deflection can be reduced by almost 65% to 90% for all thicknesses and distribution patterns considered.*

Keywords: Functionally graded material; Maximum deflection; Graphene nanoplatelets; Distribution patterns; Nanocomposite

1 INTRODUCTION

Extensive research has been conducted on the flexural analysis of Functionally Graded Material (FGM) composite plates reinforced with Carbon Nano Tubes (CNTs) in the past (Bhardwaj et al. 2013, Mehar and Panda 2016, Mohammadimehr et al. 2016, Kumar and Srinivas 2017). On the other hand, it is reported that FGM composite plates reinforced with GPLs are more advantageous in terms of deflection reduction with even a small percentage of GPL(Feng et al. 2017, Zhao et al. 2017). Chen et al. (2013) showed that a small percentage (like 1.3%) of graphene oxide and CNT nanofillers tend to increase the bending and stretching durability of nanofiller reinforced composites. FGM composite structures reinforced with GPLs were further investigated for different boundary conditions (Muni Rami Reddy et al. 2018) and flexural capacity in various areas such as beams (Feng et al. 2017), porous beams (Sahman et

al. 2017), square plates (Gholami and Ansari 2017, Song et al. 2017), trapezoidal plates (Zhao et al. 2017).

Very recently, Song et al. (2017) investigated the bending analysis of functionally graded multilayer GPL reinforced polymer composite plates using the first order shear deformation theory (FSDT). In their investigation, they considered the weight fraction of GPL to have a layer-wise variation along the thickness direction with GPLs uniformly dispersed in the polymer matrix in each individual layer. For their computations, the effective Young's modulus of the plate was predicted using the modified Halpin-Tsai model while effective mass density and Poisson's ratio were determined by the rule of mixtures. However, their investigation was limited to moderately thick plates and GPLs were distributed linearly in thickness direction and uniformly in the plan. To the best of authors' knowledge, a comprehensive investigation of the above problem that deals with GPLs distributed in plan (length and width) and GPLs distributed linearly and nonlinearly in the thickness direction for thick, moderately thick and thin plates has not been reported. This paper attempts to fill this research gap.

2 FORMULATION

A functionally graded GPL reinforced epoxy matrix composite multi-layer plate with length L, width W and thickness T, loaded with a distributed load F(X, Y) parallel to the z-axis as shown in Fig. 1 is considered. The number of layers is denoted as N_L and the thickness of each layer (T/ N_L) is the same. Each layer of the composite plate is assumed to have a uniform dispersion of GPLs in polymer matrix in x-y plane. Firstly, the percentage of GPL weight fraction is considered to be distributed along thickness direction using four different basic patterns for a simply supported in all four sides (SSSS boundary condition). The distribution 1 (D1) is the special case of homogeneous composite plate in which GPLs are distributed uniformly along the plate thickness direction. The GPL weight fraction is distributed linearly along plate thickness in a symmetric way in distributions 2 (D2) and 3 (D3) and an unsymmetrical way in distribution 4 (D4). The GPL weight fraction increases linearly from zero at the top layer to maximum at middle layer in D2 and vice versa in D3. In D4, the GPL weight fraction increases linearly from zero at the top layer to maximum at the bottom layer.

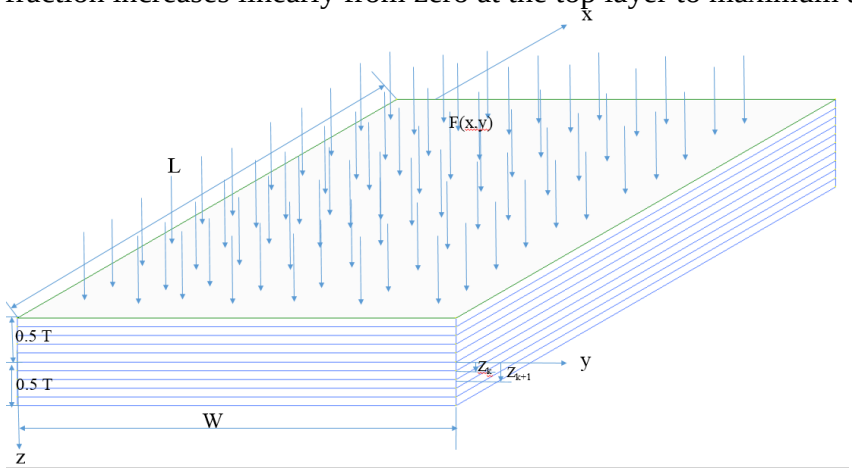

Fig. 1. Laminated multi-layer GPL/epoxy functionally graded composite plate.

The mathematical equations for distribution types1-4 are given below (Song et al. 2017). $p_{GPL}^{(k)}$ is the weight fraction of GPL in k-th layer.

Epoxy polymer: $p_{GPL}^{(k)} = 0$, D1: $p_{GPL}^{(k)} = p_{GPL}^{*}$,

$$\text{D2: } p_{GPL}^{(k)} = \frac{4 * p_{GPL}^{*}\left(\frac{N_L+1}{2} - \left|k - \frac{N_L+1}{2}\right|\right)}{(2+N_L)} \text{ , D3: } p_{GPL}^{(k)} = \frac{4 * p_{GPL}^{*}\left(\frac{1}{2} + \left|k - \frac{N_L+1}{2}\right|\right)}{(2+N_L)} \text{ , D4: } p_{GPL}^{(k)} = \frac{2 * k * p_{GPL}^{*}}{(N_L+1)} \quad (1)$$

where $k = 1, 2, 3 \ldots\ldots N_L$ which corresponds to each layer of the plate, p_{GPL}^{*} value is same for each distribution i.e. total volume of GPLs used in the plate is the same for all distribution patterns.

In addition to the above distribution patterns, higher order parabolic distribution (HOPD) type is also utilized in this research which has maximum GPL weight fraction at top and bottom layers and zero at the layers at the mid height. Other researchers attempted parabolic distributions (Yang et al. 2017). The modified equation of parabolic distribution is shown below.

$$\text{HOPD (n): } p_{GPL}^{(k)} = \frac{2^n}{T^n} \lambda\, p_{GPL}^{*}\, z^n \quad (2)$$

where $\lambda = (n+1)\sqrt{p_{GPL}^{*}}$ is weight fraction, index, n=2 for parabolic distribution and z is the distance from center of thickness to bottom and top of k^{th} layer in +ve and –ve z axes, respectively.

Channel type distributions in Thickness (TC): In this type of distribution, the thickness is divided into two parts. One part is top 2 and bottom 2 layers and other part is middle 16 layers (when N_L =20). Total volume of GPLs used in the plate is the same for all TC distribution types. However, the weight fraction of GPLs in each layer in both parts change based on TC type. The GPLs distribution into epoxy polymer matrix in sandwich/channel type of distributions TC1 to TC10 in thickness direction is explained in section 3.1. For example, TC5 means each layer in top 2 and bottom 2 layers has 4.0% of GPL and each layer of middle 16 layers has 0.25% GPL, resulting in 1% GPL total percentage for the overall plate.

Equal Area distribution in Plan (PE): The plate is divided into two equal parts of inside and outside parts as shown in Fig. 2 (a). Total volume of GPLs used in the plate is the same for all equal area distribution types. However, weight fraction of GPLs in inside part and outside are different based on each distribution type.

Mid-side equal area distributions in Plan (PM): The plate is divided into two equal area parts of sum of mid-side areas and sum of corner areas equal to centre areas as shown in the Fig 2(b). Total volume of GPLs used in the plate is the same for all PM distribution types. However, the weight fraction of GPLs in mid-side part and corner and centre part changes based on each distribution type.

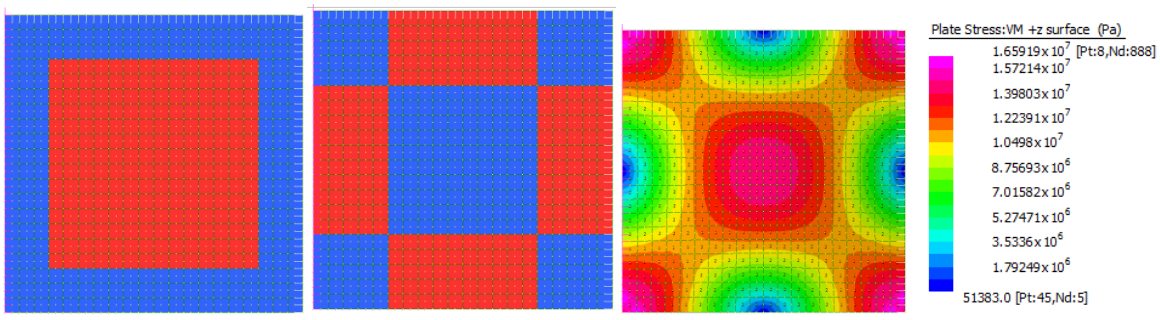

(a) Equal area pattern (b) Mid portion equal area pattern (c) Von Mises stress distribution for the plate

Fig. 2. GPLs distributed into epoxy polymer matrix in different types of distributions in length and width directions.

2.1 Effective Material Properties

The Poisson's ratio and density of FGM are calculated based on rule of mixture. The volume fraction of GPL (V_{GPL}) and volume fraction of epoxy (V_{epoxy}) are calculated as follows:

$$V_{GPL} = \frac{p}{\left[1-\frac{\rho_{GPL}}{\rho_{epoxy}}\right]p+\frac{\rho_{GPL}}{\rho_{epoxy}}}, \qquad V_{epoxy} = 1-V_{GPL} \tag{3}$$

where ρ_{GPL} and ρ_{epoxy} are densities of GPL and epoxy matrix, respectively.

The effective Young's modulus of GPL reinforced composite material (E_c) is approximated based on Voigt-Reuss model (Guzmán de Villoria and Miravete 2007).

$$E_c = \left[\left(\frac{3}{8}\right)E_L + \left(\frac{5}{8}\right)E_W\right] \tag{4}$$

where longitudinal modulus, E_L, and transverse modulus, E_W, are determined from Halpin-Tsai model (Halpin and Kardos 1976).

2.2 Governing Equation

Using the standard finite element discretization process (Huang 1989, Strand7 2005), the governing equation of motion for the bending analysis of the plate is as follows:

$$[\mathbf{K}]\{\Delta\} = \{\mathbf{F}\} \tag{5}$$

where **K** is the usual stiffness matrix and $\Delta = \{U\ V\ W\ \phi_x\ \phi_y\}$ is the generalized nodal displacement vector and **F** is the force vector**.**

In this paper, finite element software (Strand7 2005), is used to solve equation (5) for deflections. In particular, quad9 element with composite laminate is used.

3 RESULTS AND DISCUSSION

In this section, the numerical results for the flexural behaviour of reinforced FGM plate in terms of dimensionless maximum deflections are presented.

3.1 Case Study on GPL Distribution Patterns in Thickness Direction

Case study considered in this paper is a GPL reinforced square epoxy plate (0.45 m x 0.45 m) with three different L/T ratios of 5, 10 and 20. Length (l_{GPL}), width (w_{GPL}) and height (h_{GPL}) of GPL particles are taken as $2.5\mu m, 1.5\mu m$ and $1.5\,nm$, respectively (Song et al. 2017). The material properties of GPL and epoxy used as polymer matrix are given below (Yasmin and Daniel 2004, Liu et al. 2007). Total weight fraction of GPLs used in the composite plate is 1% for all D1, D2, D3, D4, HOPD and TC distribution types.

$$\nu_{GPL} = 0.186,\ E_{GPL} = 1.01\ \text{TPa},\ \rho_{GPL} = 1060\ \text{kg/m}^3,\ \rho_{epoxy} = 1200\ \text{kg/m}^3\ \nu_{epoxy} = 0.34,\ E_{epoxy} = 3.0\,\text{GPa} \tag{6}$$

$$w_{max} = \frac{W_{max}\,E_{epoxy}T^3}{12\left(1-\nu_{epoxy}^2\right)F_0\,L^4}, \qquad w_{epoxy} = \frac{W_{epoxy}\,E_{epoxy}T^3}{12\left(1-\nu_{epoxy}^2\right)F_0\,L^4}, \qquad \hat{w}_{max} = \frac{w_{max}}{w_{epoxy}}x100 \tag{7}$$

where maximum deflection, w_{max} and w_{epoxy} are dimensionless maximum deflection for plates with and without GPL, respectively. The percentage maximum deflection ratio of reinforced to unreinforced composite plate is $\hat{w}_{max}$. F_0 is the uniform lateral uniform load 500kPa (Song et al. 2017).

3.1.1. Convergence study

A convergence study on the dimensionless maximum deflection w_{max} was conducted by using different number of layers (4,6,10, 20,30 and 40) and mesh sizes (10x10, 20x20 and

30x30) for all four GPL distribution patterns D1, D2, D3 and D4 for 1%weight fraction of GPL. Table 1 shows the results and it can be concluded that 20 layers and 20x20 mesh size yielded reasonably converged results. Therefore, for the subsequent analysis, we have used 20 layers and a 20x20 mesh size.

Table 1: Convergence study on w_{max} of GPL/epoxy FGM square plate with different mesh size, distribution type (DT) and total number of layers (N_L) under a uniform load (p^*_{GPL} = 1% and L/T=10).

Mesh size	DT	N_L					
		4	6	10	20	30	40
10x10	D1	0.0991	0.0991	0.0991	0.0991	0.0991	0.0991
	D2	0.1204	0.1303	0.1396	0.1475	0.1505	0.1519
	D3	0.0841	0.0803	0.0779	0.0762	0.0758	0.0755
	D4	0.1098	0.1129	0.1157	0.1181	0.1190	0.1200
20x20	D1	0.0990	0.0990	0.0990	**0.0990**	0.0990	0.0990
	D2	0.1203	0.1302	0.1395	**0.1474**	0.1503	0.1518
	D3	0.0840	0.0803	0.0779	**0.0762**	0.0757	0.0754
	D4	0.1097	0.1128	0.1156	**0.1180**	0.1189	0.1198
30x30	D1	0.0990	0.0990	0.0990	0.0990	0.0990	0.0990
	D2	0.1203	0.1302	0.1395	0.1473	0.1503	0.1517
	D3	0.0840	0.0803	0.0779	0.0761	0.0757	0.0754
	D4	0.1097	0.1128	0.1155	0.1180	0.1188	0.1198

3.1.2. Verification of results

For verification of results, $\hat{w}_{max}$ from present method is compared in Fig. 3 with the results of Song et al.(2017) for distribution type D1, D2, D3 and D4, SSSS boundary condition in a moderately thick plate. It is seen that $\hat{w}_{max}$ decreases rapidly with small percentage of p^*_{GPL} and decreases gradually with high percentage of p^*_{GPL}. It can be seen that present results are in close agreement with reported results from the literature for D1, D2, D3 and D4 distributions.

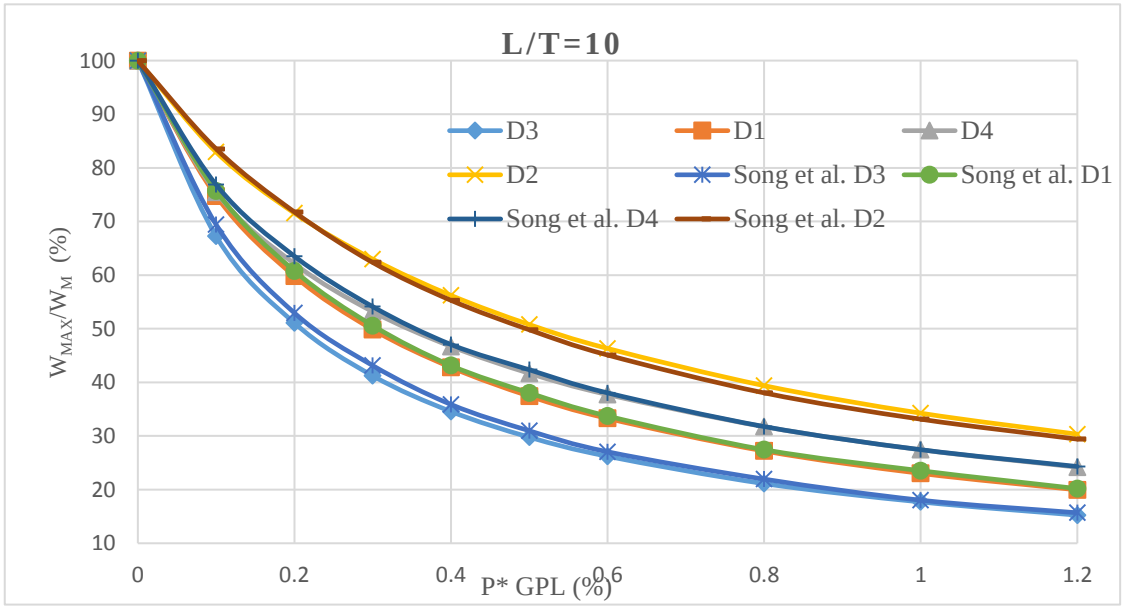

Fig. 3. The verification of results for distributions (D1-D4) for GPL/epoxy SSSS moderately thick plate.

3.1.3. Higher order parabolic distributions

Table 2 shows the results of dimensionless maximum deflection and $\hat{w}_{max}$ of the thin, moderately thick and thick simply supported composite plates for parabolic distributions of the order from 2 to 70. The higher the parabola order the larger the weight of GPL percentage in top and bottom layers and the lower the weight of GPL in middle layers with a constant total volume of GPL as per equation (2). It can be seen that the order 70, 22 and 2 are best for thin, moderately thick and thick composite plate, respectively, with low maximum deflection values. It can also be seen that there is no need of GPL reinforcement in the middle 16 layers for thin plates based on HOPD type equation (2).

Table 2: The w_{max} and $\hat{w}_{max}$ (in parenthesis) of GPL/epoxy plate with L/T=5, 10 and 20; p^*_{GPL} = 1%; N_L = 20; for HOPD (n) in thickness direction.

L/T	Epoxy	n							
		2nd	3rd	4th	8th	14th	22nd	30th	70th
10	0.4301	0.0674	0.0638	0.0617	0.0580	0.0565	0.0560	0.0561	0.0566
		(15.68)	(14.84)	(14.33)	(13.48)	(13.14)	**(13.03)**	(13.03)	(13.15)
5	0.4957	0.0941	0.0945	0.0948	0.0963	0.0978	0.0993	0.1004	0.1033
		(18.99)	(19.06)	(19.13)	(19.42)	(19.74)	(20.03)	(20.26)	(20.83)
20	0.4119	0.0607	0.0562	0.0534	0.0484	0.0462	0.0452	0.0450	0.0449
		(14.75)	(13.64)	(12.95)	(11.75)	(11.21)	(10.98)	(10.92)	**(10.89)**

3.1.4. Sandwich type or channel type distribution

Table 3 shows the results of dimensionless maximum deflection and $\hat{w}_{max}$ of the thin, moderately thick and thick simply supported composite plates for all channel type distribution types TC1 to TC10. The weight fraction of GPLs in both parts changes based on TC type as shown in Table 3. It can be seen that the channel type TC1, TC3, and TC7 is best for thin, moderately thick and thick composite plate, respectively, with them yielding the lowest maximum deflection.

The best distribution out of D1 to D4 is D3 (refer Fig 3) with $\hat{w}_{max}$ of 17.8% for moderately thick plate for 1% GPL. However, $\hat{w}_{max}$, decreases to 13.7% for TC3 and 13.03% for 22nd HOPD. It makes sense as GPLs must be distributed according to Von Mises stresses as explained in Zhao et al.(2017).

Table 3: w_{max} and $\hat{w}_{max}$ of GPL/epoxy plate with L/T=5, 10 and 20; p^*_{GPL} = 1%; N_L = 20; for channel type distributions in thickness direction.

	TC1	TC2	TC3	TC4	TC5	TC6	TC7	TC8	TC9	TC10
GPL % in top 2 and bottom 2 layers	5.00%	4.75%	4.50%	4.25%	4.00%	3.75%	3.50%	3.25%	3.00%	2.50%
GPL % in middle 16 layers	0.00%	0.0625%	0.125%	0.1875%	0.25%	0.3125%	0.375%	0.4375%	0.50%	0.625%
L/T										
10	0.0603	0.0592	**0.0589**	0.0593	0.0601	0.0613	0.0628	0.0646	0.0667	0.0719
	(14.03)	(13.77)	**(13.70)**	(13.79)	(13.98)	(14.25)	(14.60)	(15.02)	(15.51)	(16.71)
5	0.1068	0.0979	0.0921	0.0884	0.0861	0.0848	**0.0843**	0.0844	0.0851	0.0882
	(21.55)	(19.75)	(18.58)	(17.83)	(17.36)	(17.10)	**(17.00)**	(17.03)	(17.18)	(17.79)
20	**0.0487**	0.0496	0.0507	0.0520	0.0536	0.0554	0.0574	0.0597	0.0621	0.0678
	(11.82)	(12.03)	(12.30)	(12.64)	(13.02)	(13.46)	(13.95)	(14.48)	(15.08)	(16.46)

3.2 Case Study on GPL Distribution Patterns in Plan

Total weight fraction of GPLs used in the composite plate is 1% for all PE and PM distribution types in plan described in this section.

3.2.1. Equal area distribution (PE type)

The weight fraction of GPLs in inside part and outside part changes based on each equal area distribution type PE1 to PE9 in plan and D3 along thickness direction for the moderately thick plate considered in this case. The area of inside part is equal to outside part (see Fig. 2a). Table 4 shows that dimensionless maximum deflection and $\hat{w}_{max}$ decrease when weight fraction of GPL is more in inner part than in outer part. PE4 is the best combination yielding a lowest $\hat{w}_{max}$ of 16.21%. If GPL distribution changes in plan when D3 along the thickness is a constant, the $\hat{w}_{max}$, decreases from 17.77% to 16.21%.

Table 4: w_{max} and $\hat{w}_{max}$ of GPL/epoxy plate with L/T=10; p^*_{GPL} = 1% and D3 in thickness direction; N_L = 20; for equal area patterns in plan.

	PE1	PE2	PE3	PE4	PE5	PE6	PE7	PE8	PE9
p^*_{GPL}(Inner part)	1.00%	2.00%	0.00%	1.50%	1.20%	1.40%	1.60%	1.70%	1.80%
p^*_{GPL}(outer part)	1.00%	0.00%	2.00%	0.50%	0.80%	0.60%	0.40%	0.30%	0.20%
w_{max}	0.0764	0.0883	0.1575	0.0697	0.0723	0.0701	0.0699	0.0708	0.0731
$\hat{w}_{max}$	(17.77)	(20.52)	(36.61)	**(16.21)**	(16.81)	(16.30)	(16.25)	(16.47)	(16.98)

3.2.2. Mid-side equal area distributions (PM type)

Fig. 2 (c) shows the Von-Mises stress distribution in plan for epoxy polymer composite plate. The stress is almost the same for middle and the corners. Therefore, weight fraction of GPLs in mid-side part and corner and centre part are set based on each distribution type from PM1 to PM9 for moderately thick plate with thickness distribution D3. Table 5 shows that dimensionless maximum deflection and $\hat{w}_{max}$ decreases when weight fraction of GPL is more in the center and corner part than in the mid-side area part. PM9 is the best combination which yields the lowest $\hat{w}_{max}$ of 16.16% for the moderately thick plate.

Table 5: w_{max} and $\hat{w}_{max}$ of GPL/epoxy plate; p^*_{GPL} = 1% and D3 in thickness direction; N_L = 20; for mid side equal area distributions in plan.

L/T		PM1	PM2	PM3	PM4	PM5	PM6	PM7	PM8	PM9
	p^*_{GPL}(Centre and Corner)	1.00%	2.00%	0.00%	1.60%	1.40%	1.20%	1.80%	1.70%	1.50%
	p^*_{GPL}(mid side)	1.00%	0.00%	2.00%	0.40%	0.60%	0.80%	0.20%	0.30%	0.50%
5	w_{max}	0.0950	0.1190	0.2385	0.0926	0.0906	0.0915	0.0989	0.0950	0.0912
5	$\hat{w}_{max}$	(19.16)	(24.00)	(48.11)	(18.68)	**(18.28)**	(18.45)	(19.96)	(19.17)	(18.39)
10	w_{max}	0.0764	0.0829	0.2578	0.0698	0.0698	0.0719	0.0729	0.0708	0.0695
10	$\hat{w}_{max}$	(17.77)	(19.28)	(59.95)	(16.23)	(16.22)	(16.72)	(16.94)	(16.47)	**(16.16)**
20	w_{max}	0.0714	0.0724	0.1952	0.0638	0.0645	0.0670	0.0657	0.0644	0.0639
20	$\hat{w}_{max}$	(17.34)	(17.58)	(47.38)	**(15.49)**	(15.65)	(16.26)	(15.95)	(15.62)	(15.51)

4 CONCLUSION

The flexural behaviour of functionally graded composite plates reinforced with graphene nanoplatelets has been investigated using a first order shear deformation theory based finite element approach. Detailed conceptual GPL distribution patterns were investigated in plan and along thickness with a view to study their effect on the maximum deflection and percentage maximum deflection ratio of reinforced to unreinforced composite plate ($\hat{w}_{max}$). It is found that, by adding just 1% weight fraction of GPL, the maximum deflection can be reduced by almost 90% for thin plates. From the investigation, following conclusions can be drawn:

- For 1% GPL fraction, with uniform distribution in plan, $\hat{w}_{max}$ decreased from 19.16% to 17% for thick plate when thickness distribution changed from D3 to TC7 (channel distribution 7); 17.77% to 13.03% for moderately thick plate when thickness distribution

changed from D3 to 22nd parabola distribution; and 17.34% to 10.89% for thin plate when thickness distribution changed from D3 to 70th parabola distribution

- For 1% GPL fraction, with thickness direction distribution kept constant at D3, $\hat{w}_{max}$ decreased from 17.77% to 16.16% for moderately thick plate when plan distribution changed from uniform to PM9 (mid side equal area distribution 9).

REFERENCES

Bhardwaj G., Upadhyay A. K., Pandey R., Shukla K. K. (2013), "Non-linear flexural and dynamic response of CNT reinforced laminated composite plates." Composites Part B: Engineering **45**(1), 89-100.

Chen M., Tao T., Zhang L., Gao W., Li C. (2013), "Highly conductive and stretchable polymer composites based on graphene/MWCNT network." Chem Commun (Camb) **49**(16), 1612-1614.

Feng C., Kitipornchai S., Yang J. (2017), "Nonlinear bending of polymer nanocomposite beams reinforced with non-uniformly distributed graphene platelets (GPLs)." Composites Part B: Engineering **110**, 132-140.

Gholami R., Ansari R. (2017), "Large deflection geometrically nonlinear analysis of functionally graded multilayer graphene platelet-reinforced polymer composite rectangular plates." Composite Structures **180**, 760-771.

Guzmán de Villoria R., Miravete A. (2007), "Mechanical model to evaluate the effect of the dispersion in nanocomposites." Acta Materialia **55**(9), 3025-3031.

Halpin J.C., Kardos J. L. (1976). "The Halpin-Tsai equations: a review." Polymer Engineering & Science **16**(5), 344-352.

Huang H.C. (1989), Static and Dynamic Analysis of Plates and Shells-Theory, Software and Applications.

Kumar P., Srinivas J. (2017), "Vibration, buckling and bending behavior of functionally graded multi-walled carbon nanotube reinforced polymer composite plates using the layer-wise formulation." Composite Structures **177**, 158-170.

Liu F., Pingbing M., Ju L. (2007), "Ab initiocalculation of ideal strength and phonon instability of graphene under tension." Physical Review B **76**(6).

Mehar K., Panda S. K. (2016), "Free Vibration and Bending Behaviour of CNT Reinforced Composite Plate using Different Shear Deformation Theory." IOP Conference Series: Materials Science and Engineering **115**, 012014.

Mohammadimehr M., Salemi M. Rousta N.B. (2016), "Bending, buckling, and free vibration analysis of MSGT microcomposite Reddy plate reinforced by FG-SWCNTs with temperature-dependent material properties under hydro-thermo-mechanical loadings using DQM." Composite Structures **138**, 361-380.

Muni Rami Reddy R., Karunasena W., Lokuge W. (2018), "Free vibration of functionally graded-GPL reinforced composite plates with different boundary conditions." Aerospace Science and Technology.**78,** 147-156.

Sahmani S., Aghdam M.M., Rabczuk T. (2017), "Nonlinear bending of functionally graded porous micro/nano-beams reinforced with graphene platelets based upon nonlocal strain gradient theory." Composite Structures, 186, 68-78.

Song M., Yang J., Kitipornchai S. (2017), "Bending and buckling analyses of functionally graded polymer composite plates reinforced with graphene nanoplatelets." Composites Part B: Engineering 134, 106-113.

Strand7 (2005). "Strand7 Theoretical Manual." (2.3), 1-399.

Yang B., Kitipornchai S., Yang Y.F., Yang J. (2017), "3D thermo-mechanical bending solution of functionally graded graphene reinforced circular and annular plates." Applied Mathematical Modelling **49**, 69-86.

Yasmin A., Daniel I.M. (2004), "Mechanical and thermal properties of graphite platelet/epoxy composites." Polymer **45**(24), 8211-8219.

Zhao Z., Feng C., Wang Y., Yang J. (2017), "Bending and vibration analysis of functionally graded trapezoidal nanocomposite plates reinforced with graphene nanoplatelets (GPLs)." Composite Structures **180**, 799-808.